

Simulation of thermoluminescence signals at very low dose rates and low doses: Implications for dosimetric applications

George Kitis^{a,*}, Vasilis Pagonis^b

^a Aristotle University of Thessaloniki, Nuclear Physics Laboratory, 54124 - Thessaloniki, Greece

^b McDaniel College, Physics Department, Westminster, MD 21157, USA

ARTICLE INFO

Keywords:

TL simulation
Low dose TL
Electron trap lifetime
Low dose lifetime
TL peak height superlinearity

ABSTRACT

During luminescence dosimetry applications, samples are irradiated in the laboratory with irradiation dose rates of the order of 0.1 Gy/s. By contrast, samples in nature are irradiated with a dose rate many orders magnitude smaller, typically 1 mGy/year. In this paper, the effect of very low dose rates and also low doses on thermoluminescence (TL) signals is investigated using the basic one-trap one-recombination center model (OTOR). The simulations showed that at very low dose rates the assumptions of quasi-equilibrium conditions (QE) are violated. This violation of QE conditions results in a significant distortion of the shapes of TL glow curves, with the result that the peak shape methods of analysis fail to produce the correct activation energy E of the traps. At the same time, the estimated half-life of the electrons traps is found to increase significantly at very low doses. The dose response of the sample at very low dose rates is simulated for both the irradiation stage and the subsequent heating stage. The dose response of the integrated TL signal is found to coincide with the dose response during the irradiation stage. However, the TL dose response measured in terms of the peak height shows a significant under-response at very low doses, making the whole dose response curve superlinear before the onset of saturation. The peak height under-response is due to the clear violation of QE conditions at very low doses and dose rates. The reported distortion of the TL glow curves and the existence of superlinearity of the TL signals at low dose rates, have important implications for the analysis of TL signals. Researchers need to be aware of the possibility that both of these effects may be present, since they can influence the analysis of experimental data and can lead to the wrong conclusions in dosimetric applications.

1. Introduction

During luminescence dosimetry applications, samples are irradiated in the laboratory with irradiation dose rates of the order of 0.1 Gy/s. By contrast, samples in nature are irradiated with a dose rate many orders magnitude smaller, typically with 1 mGy/year. This difference of several orders of magnitude between the natural and laboratory dose rates can have important implications for the luminescence signals commonly used for luminescence dosimetry and luminescence dating.

In this paper we use the simplest phenomenological model of thermoluminescence, which is based on one-trap and one-recombination center (OTOR). This model, under certain conditions, leads to the commonly used first order kinetics model (Randall and Wilkins, 1945a,b), second order kinetics (Garlick and Gibson, 1948) and general order kinetics (May and Partridge, 1964). The OTOR model has been studied extensively, and several analytical equations have been developed for the TL signals from dosimetric materials (Kitis and Vlachos, 2013; Lovedy Singh and Gartia, 2013; Sadek et al., 2014).

Within the OTOR model, significant competition can take place between recombination and retrapping energy transitions of the available electron traps and holes. The current paper studies these competition phenomena at low dose rates and low doses.

From the practical point of experimental studies, the dependence of the TL signal on irradiation dose has an experimental threshold, termed the lowest detectable limit (LDL). The TL dose response curve (DRC) is known experimentally only at doses greater than the LDL. However, TL production also takes place for doses less than the LDL. The question of how very low dose rates affect the dose response below the LDL can only be answered by simulations. For this purpose, we study the dose response over many orders of magnitude of the irradiation dose.

The results of the simulations can help researchers understand better TL signals which involve very low dose rates, as in the case of archaeological and geochronological TL dating. For example, when a ceramic is extracted from a furnace, or a geological material is bleached by sunlight, the traps responsible for luminescence signals are assumed

* Corresponding author.

E-mail address: gkitis@auth.gr (G. Kitis).

to be empty, and the sample starts being irradiated with extremely low dose rates, possibly arriving at their LDL dose values after decades, hundreds, or even thousands of years. Therefore, understanding the (theoretical) TL dose response below the LDL limit is an important piece of information while analyzing TL signals measured in the laboratory.

The goals of the simulations in the present works are:

- To simulate and analyze the TL signals within the OTOR model, under conditions of very low dose rate and low doses.
- To investigate whether the quasi-equilibrium conditions (QE) and the well-known methods of TL peak shape analysis are applicable under these conditions.
- To simulate the filling of electron traps under these, conditions and obtain the corresponding TL dose response over several orders of magnitude of the irradiation dose.
- To estimate theoretically the effects of trap filling on the half-life of the trapped electrons and on the thermal stability of traps.

2. The one trap one recombination center (OTOR) phenomenological model

Fig. 1 shows the energy bands and processes being simulated in the OTOR model. The simulations consist of three stages, termed (i) irradiation stage, (ii) relaxation stage and (iii) heating stage.

The differential equation governing the traffic of electrons and holes in this model are the following.

$$\frac{dT}{dt} = \beta \tag{1}$$

$$\frac{dn}{dt} = ns e^{-\frac{E}{kT}} + A_n(N - n)n_c \tag{2}$$

$$\frac{dm}{dt} = A_h(M - m)n_v - A_m m n_c, \tag{3}$$

$$\frac{dn_v}{dt} = Drate - A_h(M - m)n_v, \tag{4}$$

$$\frac{dn_c}{dt} = Drate - \frac{dn}{dt} - A_m m n_c, \tag{5}$$

Where E (eV) is the activation energy, s (s^{-1}) the frequency factor, N (cm^{-3}) is the concentration of available electron traps, n (cm^{-3}) the concentration of trapped electrons, M (cm^{-3}) is the concentration of available luminescence centers, m (cm^{-3}) is the concentration of trapped holes, n_c (cm^{-3}) and n_v (cm^{-3}) are the concentrations of electrons in the conduction and holes in the valence band, A_n ($cm^3 s^{-1}$) is the trapping coefficient in electron trap, A_m ($cm^3 s^{-1}$) is the recombination coefficient, A_h ($cm^3 s^{-1}$) the trapping coefficient of holes in luminescence centers, β (K/s) the heating rate and $Drate$ is the rate of production of ion pairs (ip) per second and per unit volume (ip $s^{-1} cm^{-3}$).

Eq. (1) evaluates the time variation of the temperature of the sample, while Eqs. (2)–(5) express the time variation of the concentrations $n(t)$, $m(t)$, $n_v(t)$ and $n_c(t)$ respectively.

The ratio n_0/N of the concentrations of trapped electrons at the end of irradiation (n_0) and of available electron traps (N) is a quantity with a key role in the present simulations.

The simulation follows closely the three physical processes shown in Fig. 2, for the irradiation, relaxation and heating stages. During the irradiation stage, the initial values of the parameters are sample temperature $T_0 = 273$ K, heating rate $\beta = 0$ K/s and all concentrations $n_{10} = 0$, $n_{20} = 0$, $m_0 = 0$, $n_{c0} = 0$, $n_{v0} = 0$. The dose rate in the present work was taken as $Drate = 10^3 (e-h)$ pairs/s/cm³, as discussed later in this paper. The values of the concentrations at the end of the irradiation stage are used as input values for the relaxation stage.

During the relaxation stage, one uses $\beta = 0$ and $Drate = 0$, since there is no sample heating or irradiation. The values of the concentrations at the end of the relaxation stage are used as input values for the heating stage.

During the heating stage we set $Drate = 0$ and $A_h = 0$, since there is no irradiation and hole trapping taking place. The heating rate is

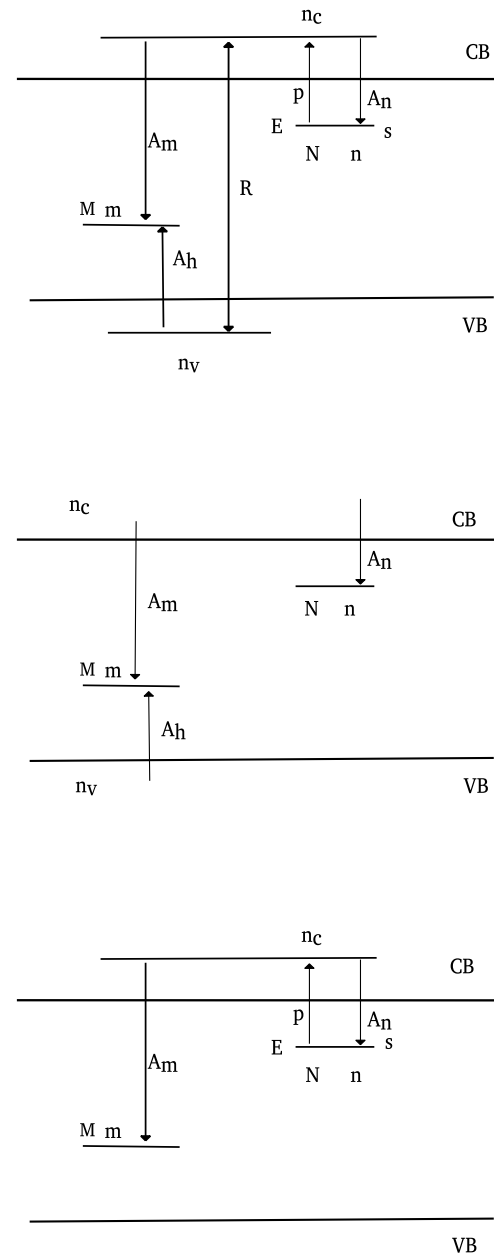


Fig. 1. The energy band model for the OTOR model, showing the irradiation stage (a), relaxation stage (b) and heating stage (c).

taken as $\beta = 1$ K/s. At the end of the heating stage the TL glow peak is obtained.

It must be emphasized that, as was shown by Sadek and Kitis (2017), it is necessary that all simulations of luminescence signals contain all three stages described above, in order to produce physically reasonable results.

The simulations consist of solving the above system of ordinary differential equations (ODEs), using the standard Scientific Python (SciPy) package in the Python programming language.

3. Methods of analysis of the results from the model

In this section we will describe the methods of analyzing the simulated results.

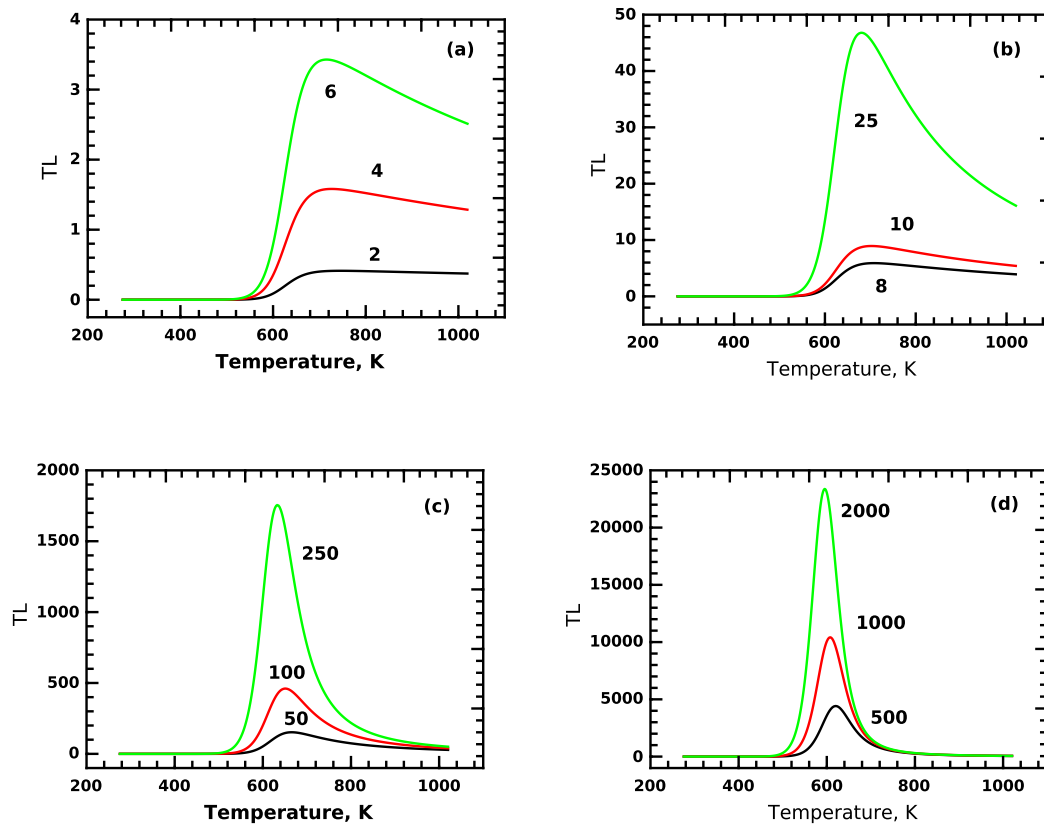


Fig. 2. Simulated TL peak shapes as a function of irradiation time in the range 2–200 s. The numbers on the peaks represent the irradiation times in seconds, so that the curve labeled 2 corresponds to an irradiation time of 2 s.

3.1. The peak shape methods (PSM) for evaluating the activation energy E

The simulated TL glow curves are analyzed using the well-known peak shape methods, in order to evaluate the activation energy E characterizing the trap.

In the present work we apply the generalized Chen equations (Chen, 1969; Kitis and Pagonis, 2007; Kitis et al., 2008; Kitis, 2020), which allow the simultaneous evaluation of the kinetic order b and the energy E . These equations are based on the following geometrical characteristics of the TL glow curves:

n_0 : The integrated signal of the simulated TL peak

n_m : The integrated signal of the high temperature part of the peak, above the temperature of maximum intensity.

I_m, T_m : The intensity I_m and the temperature at the peak maximum T_m

T_1, T_2 : The temperature at the low and at high temperature side of the peak, at the half intensity $I_m/2$

ω, τ, δ : The full width of the peak $\omega = T_2 - T_1$, and the half-widths on the low and high temperature side of the peak, $\tau = T_m - T_1$ and $\delta = T_2 - T_m$ respectively.

μ_g, μ'_g : The geometrical shape symmetry factor $\mu_g = \delta/\omega$ and the integral symmetry factor $\mu'_g = n_m/n_0$ correspondingly.

Once the above parameters are evaluated, the next step is to evaluate the triangle assumption pseudo-constant C_ω which, is defined as the degree by which the integral n_0 of the simulated TL peak approximates

the area of a triangle with height I_m and base 2ω . It is given by the expression

$$C_\omega = \frac{\omega I_m}{\beta n_0} \quad (6)$$

By using the values of μ'_g, T_m, E we can evaluate the kinetic order b of the luminescence process to any desired accuracy, using the iteration method based on the equation:

$$\mu'_g = \left[\frac{b}{1 + (b-1) \frac{2kT_m}{E}} \right]^{-\frac{1}{b-1}} \quad (7)$$

Finally, the value of the activation energy E can be evaluated using the pseudo-constant C_ω and the evaluated kinetic order b , through the equation:

$$E_\omega = C_\omega \frac{b}{\mu'_g} \cdot \frac{k T_m^2}{\omega} \quad (8)$$

3.2. The half-life of a trap in the OTOR model

In the present simulation, the thermal stability of the energy level corresponding to the TL peak is of crucial importance, since it is directly related to the luminescence process, and it depends strongly on the trap occupancy n_0/N at the end of the irradiation process. As a measure of the thermal stability of the trap, we use the half-life $\tau_{1/2}$ for an isothermal decay process. For the purposes of this paper, the half-life $\tau_{1/2}$ is defined as the time required for the population of the trapped charge in a single trap to decay to half its initial value. Kitis and Pagonis (2017) derived a general expression for the half-life of a TL trap, in the framework of the OTOR model. The general expression of the half-life depends on the kinetic parameters E, s of the trap, on the trap filling

ratio n_0/N and on the retrapping coefficient $R = A_n/A_m$, which is the ratio of the retrapping and recombination coefficients A_n and A_m :

$$\tau_{1/2} = \frac{1}{\lambda} \left\{ \frac{NR}{n_0} + (1-R) \ln 2 \right\} \quad (9)$$

where

$$\lambda = s \exp\left(-\frac{E}{kT}\right) \quad (10)$$

The importance of this equation is that it allows us to estimate the half-life of the trap at very low doses represented by the low trap filling ratio n_0/N .

In addition to using Eq. (9), we can also estimate the half-life of the trap using the empirical general order kinetics (GOK). The half-life expression for general order kinetics was given by Furetta and Kitis (2004), as

$$(\tau_{1/2})_{GOK} = \frac{1}{\lambda} \left\{ \left(\frac{n_0}{N}\right)^{1-b} \frac{1}{1-b} \left(1 - \frac{1}{2^{1-b}}\right) \right\}, \quad b \neq 1 \quad (11)$$

where $1 < b \leq 2$ is the kinetic order. Note that the empirical general order kinetics parameter b corresponds to the phenomenological OTOR model parameter R . For first order kinetics one has $R \ll 1$ or $b = 1$, and one obtains the well known expression for lifetime (Randall and Wilkins, 1945a), which is widely used by the TL community:

$$\tau_{1/2} = \frac{1}{\lambda} = s^{-1} \exp\left(\frac{E}{kT}\right) \quad (12)$$

For second order kinetics these equations apply for $R = 1$ and $b = 2$.

3.3. Correspondence between irradiation dose and the rate of production of ion pairs

The physical unit of dose is the Gy, which unfortunately cannot be used directly in simulations of phenomenological models. In these models the dose and dose rate units are given in terms of the number of ion pairs $Drate$ produced per unit time and per unit volume (ip $s^{-1} cm^{-3}$). Similarly, the dose in these models is derived as the product of $Drate$ and the irradiation time, during the irradiation stage of the simulation. Therefore, in simulations the dose is in units of ion pairs produced per unit volume (ip cm^{-3}). For simplicity, we assume a sample with a volume of $1 cm^3$, so that the irradiation doses in the figures of this paper are reported simply in units of ip.

The relationship between the dose in Gy and the dose rate parameter $Drate$ was discussed in the book by Chen and Pagonis (2011), their Chapter 8. These authors considered the example of LiF, and used the density of this material and an average energy of 36 eV required for the production of an electron-hole pair. Starting from the definition of $1 Gy = 1 J kg^{-1}$, they estimated the number of electron-hole pairs produced when 1 Gy is delivered to the sample. They concluded that a laboratory dose rate value of $Drate = 10^{12} ip cm^{-3} s^{-1}$ corresponds to an actual dose rate of $0.03 Gy s^{-1}$.

The natural irradiation dose rate will be about 8 orders of magnitude smaller, with a value of $Drate = 10^4 ip cm^{-3} s^{-1}$ corresponding to an actual dose rate of approximately $10^{-12} Gy s^{-1}$ (or approximately $1 mGy y^{-1}$).

On the basis of this previous estimate, we use a very low natural dose rate $Drate = 10^3 ip cm^{-3} s^{-1}$ in the simulations of this paper.

3.4. Choosing the extent of the irradiation doses

Let us consider the well known experimental dose response region of the common TL material LiF(TLD-100), which varies approximately between 1 mGy and 10 Gy, i.e. it covers a region of four orders of magnitudes. On the basis of these estimates, we consider that the measurable experimental dose region usually extends over 4–5 orders of magnitudes.

In addition, we assume that the above experimental dose response region extends in reality below the LDL, by several more orders of

magnitude. We also use a saturation dose of 10^{10} – $10^{12} ip cm^{-3}$. These numerical values determine the extent of the irradiation in the simulation. These irradiation times should be appropriate for the simulation of the dose response below the LDL.

However, it is noted that it is not strictly necessary to predefine an LDL threshold in the model, and the results reported here should be applicable for a variety of dosimetric materials.

3.5. The QE conditions

The quasi-equilibrium conditions (QE) are a fundamental set of assumptions usually made in phenomenological luminescence models. One of the main goals of this paper is to test whether the QE assumptions are valid under the conditions of low dose rates and low doses used in the simulations.

The QE assumptions are usually stated as the inequalities:

$$\left| \frac{dn_c}{dt} \right| \ll \left| \frac{dn}{dt} \right|, \left| \frac{dm}{dt} \right| \quad n_c \ll n \quad (13)$$

In the simulations of this paper, we follow the concentrations n_c, n, m as well as their derivatives, and investigate whether the QE conditions are violated.

A detailed discussion and mathematical description of the QE assumptions was carried out by Chen and Pagonis (2013). These authors showed that using a certain set of parameters in the OTOR model, these conditions are not satisfied. In addition, they showed that instead of Eq. (13), one can evaluate the following two terms during the simulation:

$$Term_1 = s \exp[-E/(kT)] \quad (14)$$

$$Term_2 = A_n(N - n)n_c + A_m m n_c \quad (15)$$

and the QE conditions can be expressed as the inequality:

$$\left| \frac{dn_c}{dt} \right| \ll Term_1, Term_2 \quad (16)$$

The physical meaning of this equation is that the rate of change dn_c/dt of the concentration of electrons in the conduction band, should be smaller than the rate of addition of electrons ($Term_1$), and also smaller than the rate of subtraction of electrons from the conduction band ($Term_2$).

4. Simulation results and discussion

4.1. The effect of low dose rate on the shape of TL glow curves

The input parameters in the simulation were $N = M = 10^{10} cm^{-3}$, $E = 1.5 eV$, $s = 10^{13} s^{-1}$, $A_h = 10^{-7} cm^3 s^{-1}$, $A_n = 10^{-9} cm^3 s^{-1}$ and $A_m = 10^{-7} cm^3 s^{-1}$. In this case the retrapping to recombination ratio is $R = A_n/A_m = 0.01$. This R value corresponds, normally, to first order kinetics.

The simulation was repeated once more with all the parameters being the same, except we set $A_n = A_m = 10^{-7} cm^3 s^{-1}$, which corresponds to second order kinetics ($R = 1$). Our purpose here was to examine whether the order of kinetics will affect the results of the simulation.

As discussed above, the irradiation dose rate was $Drate = 10^3 ip s^{-1} cm^{-3}$ and the irradiation time from 2 – $10^8 s$, so that the lowest dose was $2 \times 10^3 ip cm^{-3}$ and the highest possible dose was $10^{11} ip cm^{-3}$. These values cover a dose region of eight orders of magnitude, which should include doses well below the LDL.

The shapes of single OTOR peaks at very low trap occupancy n_0/N (i.e. very low dose), are shown in Fig. 2. The numbers shown on the curves are the irradiation times in seconds. For example, the TL peak in Fig. 2(a) marked as “2” results from an irradiation time of 2 s. This corresponds to a value of $n_0/N = 10^{-7}$, i.e. there is a large number of empty electron traps at the end of the irradiation.

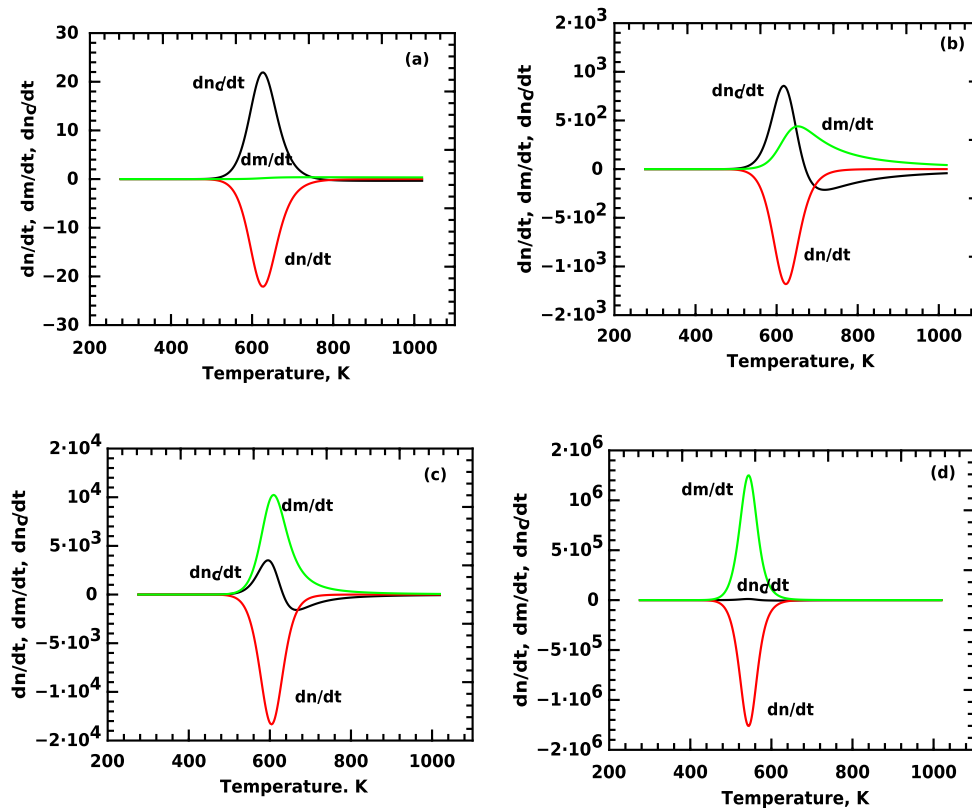


Fig. 3. The simulated rates of change of concentrations dm/dt , dn_c/dt , dn/dt during the heating stage, for different irradiation times t of (a) 2 s, (b) 100 s, (c) 1000 s (d) 10000 s. The QE conditions from Eq. (13) are clearly violated for cases (a),(b) and they apply to case (d).

During thermal stimulation an electron is released into the conduction band, and can either recombine with one of the holes or be retrapped in the electron traps. Due to the large number of available empty electron traps, at this low dose level the electrons will undergo a large number of thermal release and retrapping cycles, before they recombine with a hole. The result of this behavior is the very unusual shape of the TL peaks shown in Figs. 2(a),(b). The important observation here is that the TL peak becomes very broad at its high temperature part. The physical reason is that due to the large number of release — retrapping cycles, the recombination process is delayed significantly.

As the dose increases in Figs. 2(c,d), the recombination term $A_m m n_c$ starts to compete effectively with the retrapping term $A_n (N - n) n_c$, so that the shape of the TL glow curves becomes gradually the more familiar TL peak shape.

It is noted that this type of very broad high temperature tail in the glow curves has been reported in several dosimetric materials, with the relevant experimental results summarized in Chen and Pagonis (2013). These authors discussed in detail the behavior of the TL signal at high temperatures in these types of glow curves.

4.2. Are the QE assumptions valid at very low dose rates and low doses?

In order to test the validity of the QE conditions, the simulations evaluate the time variation of the electron concentrations at the very low doses. This is shown by plotting the concentrations dn_c/dt , dn/dt , dm/dt as shown in Fig. 3(a)–(d), for four irradiation doses of 2, 100, 1000, 10^5 s respectively.

Fig. 3 is very similar to the results obtained previously in the study by Chen and Pagonis (2013), their Fig. 3.

Fig. 3(a) describes the situation for the very low dose of 10^3 ip with $n_0/N = 10^{-7}$. In this case the rate of change of concentration of holes dm/dt in the recombination center is zero, and the corresponding rates for trapped electrons $|dn/dt|$ and conduction band electrons $|dn_c/dt|$

are practically the same. This is a clear violation of the QE condition in Eq. (13).

Fig. 3(b) describes the situation for the very low dose of 10^5 ip with $n_0/N = 10^{-5}$. At this dose a number of traps are occupied, and the retrapping rate decreases, while the recombination rate increases. However, the rate $|dn_c/dt|$ is still high compared to $|dn/dt|$, which means that the QE condition is still violated.

Fig. 3(c) describes the situation for the dose of 10^6 ip with $n_0/N = 10^{-4}$. In this case we start seeing the recovery of the QE conditions, with the rate $|dn_c/dt|$ becoming smaller than $|dn/dt|$. It is interesting that this recovery starts at least three order of magnitude before saturation, coinciding with the useful range of experimental irradiation doses in a typical dosimetric material.

Fig. 3(d) describes the situation for the dose of $6 \cdot 10^8$ ip. In this case the recombination rate dominates and the rate dn_c/dt tends to zero, indicating that the QE conditions now hold true.

The above simulation for $R = 0.01$ (normally first order kinetics) was repeated by setting $R = 1$ (normally second order kinetics) and by keeping all other parameters the same. The simulation results were very similar to those presented in Fig. 3 and are not shown here. So, it is concluded that the kinetic order of the process does not affect the results of the simulations in this paper.

4.3. The peak shape methods of evaluating e

The peak shape method of estimating the activation energy E of the electron trap was described above. In addition to the PSM, we also estimate the value of E using the empirical GOK model based on Eq. (8). In the present two simulations the values of the retrapping ratio are $R = 0.01$ and $R = 1$, which correspond to $b \sim 1$ and $b = 2$.

The output values of E and b are shown in Fig. 4(a) for $R = 0.01$, and in Fig. 4(b) for $R = 1$. At the very low doses shown in Fig. 2a, the peak shape of the glow curve is not complete and the estimated value

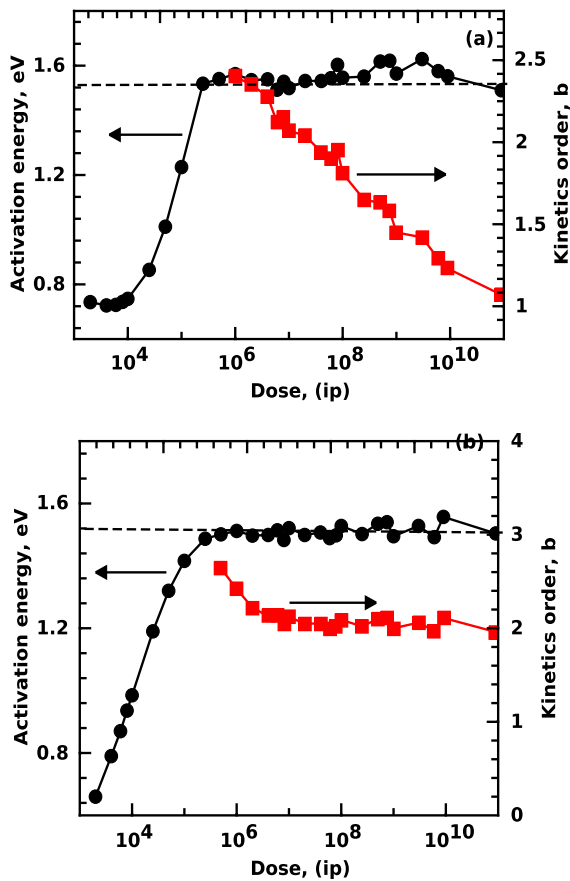


Fig. 4. (a) The values of the kinetic order b and the output values of the activation energy E , evaluated using the method described in Section 3.1, and for the TL glow curves shown in Fig. 2 where $R = 0.01$. (b) The same simulation for $R = 1$.

of b is unreliable, so that the corresponding values of E are much lower than the input $E = 1.5$ eV value. The failure of the PSM is obviously due to the distortion of the TL glow curves, caused by the violation of the QE conditions.

As the dose increases and the QE conditions recover, the PSM become more reliable and the model value of $E = 1.5$ eV is obtained within less than 2%.

In Fig. 4(a) the kinetic order b is greater than 2 at very low doses, and starts decreasing gradually towards the expected value of $b \sim 1$. However, in Fig. 4(b) the evaluated kinetic order b decreases slightly from $b = 2.6$ to a constant value of $b = 2$ in the high dose region.

The unusual large values of b shown in Fig. 4 are obtained only when the QE conditions are violated.

A strict conclusion from Fig. 4 is that when $R \ll 1$ then at low doses an OTOR peak starts always as a non first order. The first order kinetics in OTOR appears only at the boundary conditions of $A_n \ll A_m$ at $n_0 \rightarrow N$. On the other hand when, $R = 1$ the OTOR peak starts from very high b values tending to the value of $b = 2$ for a broad dose region (i.e. from $\sim 10^{-5} < n_0/N \sim 1$)

4.4. Dose response curves (DRC)

The number of trapped electrons n_0 at the end of irradiation stage, and the dose response of the TL signal are two important simulation outputs.

Figs. 5(a)(b) show the dose response behavior for a peak with parameters $E = 1.5$ eV, $s = 10^{13} \text{ s}^{-1}$, $R = 0.01$ ($b \sim 1$) and $R = 1$, ($b = 2$) correspondingly. All curves (1,2,3) are normalized to the TL at the highest (saturation) dose.

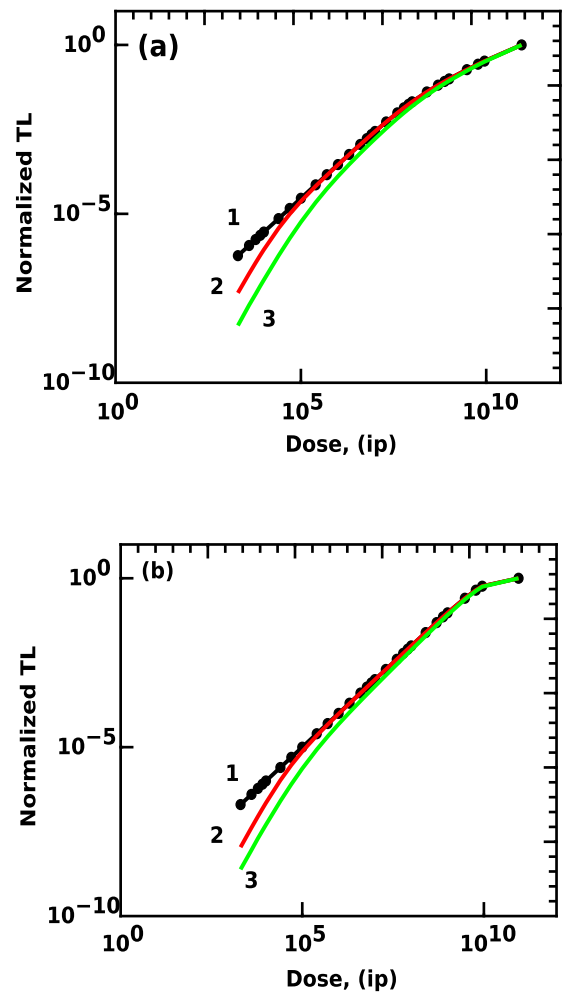


Fig. 5. Curve 1: The normalized dose response of the trapped electrons at the end of the irradiation stage (n_0). Curve 2: the corresponding dose response for the area under the TL curves. Curve 3: The corresponding dose response of the maximum TL signal I_{max} . In sub-figure (a) the retrapping ratio is $R = 0.01$, and in (b) $R = 1$.

In both figures, curve (1) represents the DRC of electrons trapped at the end of irradiation stage (n_0). Curve (2) represents the corresponding integrated TL signal obtained from Fig. 2. In the OTOR model, curves (1) and (2) should coincide, however we observe that this does not happen in the very low dose region. This disagreement at low doses is not real but artificial. It is due to a limitation of the simulation to record the whole TL peak, although, the simulation temperature was extended up to 1100 K. If the simulation was extended to even higher temperatures then curve (2) had to coincide with curve (1).

In both Figs. 5(a)(b), curve (3) represents the dose response of the TL intensity I_m at the peak maximum. The agreement between curves (1) and (3) is achieved only at high doses, due to the distortion of the shape of the glow curve at low doses. The deeper physical reason for the difference between curves (1) and (3) is once more the violation of the QE conditions.

This distortion of the glow peaks and the resulting nonlinear dose response was also reported by Chen et al. (1983) and Chen et al. (2010), who studied the nonlinear response of TL and OSL signals within the OTOR model.

Fig. 6(a)(b) is obtained by plotting the un-normalized simulated DRC curves (1) and (3) from Fig. 5(a)(b). The DRC for the concentration n_0 is clearly linear, whereas the DRC for the peak height I_{max} shows a surprising behavior of strong superlinearity. This nonlinear behavior could

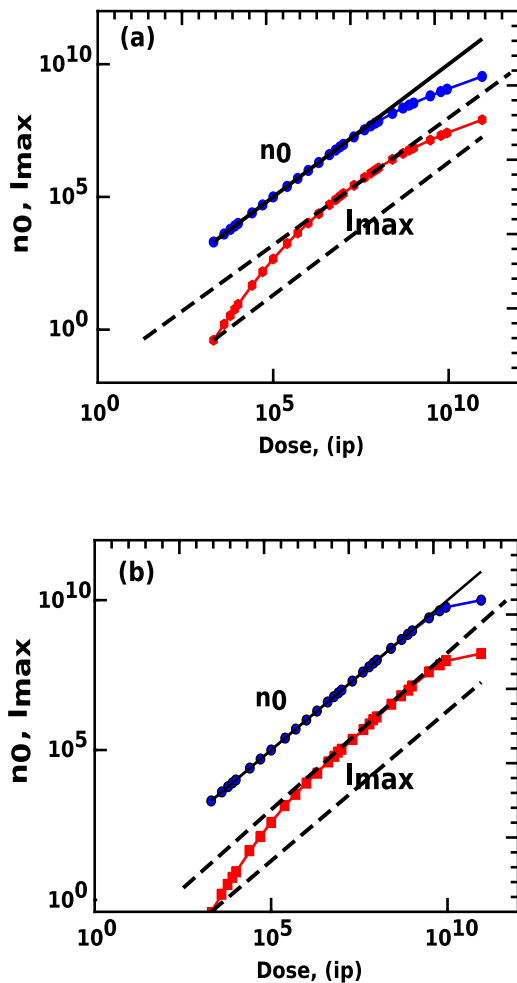


Fig. 6. The un-normalized curves 1 and 3 from Fig. 5 showing the superlinear dose response of the I_{max} signal, and the linear dose response of n_0 . The parallel lines show the linear range of the dose response.

have serious implications for applications, and needs some additional explanation as follows.

Let us consider the triangle pseudo-constant of Eq. (6). According to Eq. (6), the quantities I_m and n_0 are proportional to each other, if the full width ω of the glow curve remains the same. In the present simulations in Fig. 2, the full width ω varies dramatically. Specifically the width ω increases significantly as the dose decreases, causing a strong decrease of I_m . As the QE condition recovers, the values of ω recover too, and the proportionality between I_m and n_0 is established again. This is noted by the lines drawn in Fig. 6(a)(b), which are parallel with the lines of a linear DRG.

4.5. Half-life estimates of the trap

With the model parameters listed above, the half-life of the trap is evaluated using Eq. (9), as well as using the GOK Eq. (11) for comparison purposes.

Both estimates of the half-life depend on the trap filling ratio n_0/N , i.e. on the irradiation dose. The behavior of $\tau_{1/2}$ as a function of dose is shown in Fig. 7(a) for the case of $R = 0.01$ (first order kinetics), and in Fig. 7(b) for the case $R = 1$ (second order kinetics). In both figures the horizontal line represents the τ value at saturation ($n_0/N = 1$).

In the case $R = 0.01$ shown in Fig. 3(a), the half-life at the lowest irradiation dose is two orders of magnitude higher than the half-life at the saturation dose. This is an impressive result, which can

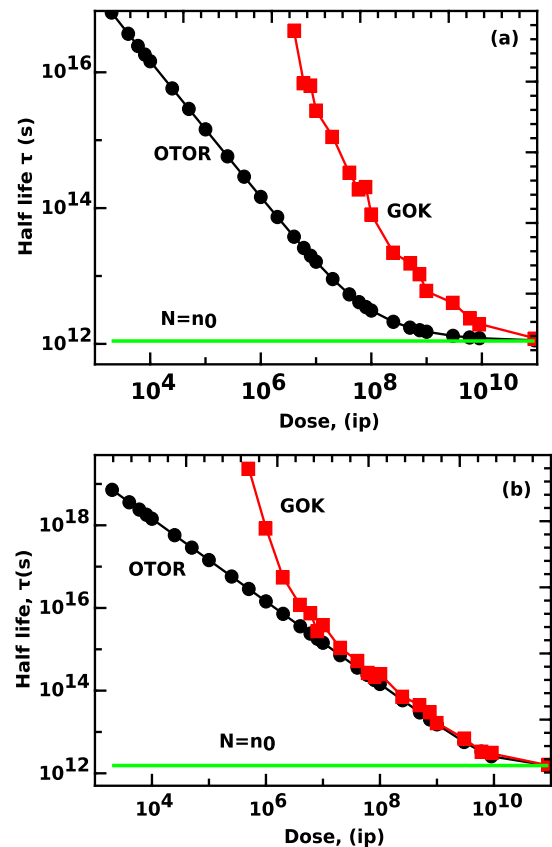


Fig. 7. Comparison between Eqs. (11) and (12), expressing the half-life as a function of trap occupancy n_0 . (a) Evaluation for $R = 0.01$, (b) Evaluation for $R = 1$.

nevertheless be understood according to the previous discussion in this paper. In the low dose region, almost all available electron traps are empty, and therefore the probability of retrapping prevails. This leads to a significantly larger apparent value of $\tau_{1/2}$. However, as the dose increases, more traps are filled and the $\tau_{1/2}$ decreases, approaching the values of τ at saturation.

The same qualitative behavior is also evaluated for the empirical GOK model using Eq. (11). However, there is a strong quantitative differentiation, due to the fact that in the GOK model the $\tau_{1/2}$ depends on both the trap filling ratio n_0/N and on the kinetic order b . As was described in Section 3, the kinetic order b is evaluated from the TL peak using the PSM. As it is seen in Fig. 2(a,b), the TL peaks have a very extensive high temperature part, which corresponds to b values much greater than $b = 2$. As the dose increases and the high temperature part of the peak recovers, the value of b decreases, and the corresponding half-life approaches that saturation limit defined by the horizontal line.

For the parameters used in this paper, the trap is thermally stable at room temperature, and its half-life at 300 K is $\tau_{1/2} = 1.1 \times 10^{12}$ s (about 3.5×10^4 yrs). The simulations show that at low doses, the effective half-life can be two orders of magnitude larger than this value.

In future work we plan to investigate the dose response as a function of the irradiation temperature in the sample's environment, especially for geological applications.

5. Conclusions and implications for applications

In this work, the behavior of an OTOR model peak was simulated under conditions of low dose rates and low doses which extend below the LDL of a typical dosimetric material.

The shape of the TL glow curve under these conditions becomes very distorted and a long high temperature tail is observed together with a shift of the TL peak towards higher temperatures. At low doses an OTOR peak starts always as a non first order. The first order kinetics in OTOR peak appears only at the boundary conditions of $A_n \ll A_m$ at $n_0 \rightarrow N$.

An important result of the simulations is that the peak shape methods of evaluating the kinetic parameters E fail, due to the distorted peak shapes. The underlying physical reason for the failure of the PSM is the failure of the QE conditions, which were tested by simulating the rates of change of the concentrations in the model ($dn/dt, dm/dt, dn_c/dt$).

This failure of the PSM can be used by researchers as a criterion for the detection of violations of the QE condition. For example, if the E value from the PSM differs significantly from the value of E obtained from the initial rise method, this may well be an indication of the failure of the QE conditions, and further study is warranted.

The simulated dose response of the trapped electrons n_0 at the end of irradiation stage is found to be linear, tending to sub-linear, and eventually approaching saturation.

Theoretically, the simulated dose response of the *integrated* TL signal during the heating stage should coincide with the dose response of n_0 . However, an under-response is observed at very low doses in the simulation, due to the strong shift of the TL peak towards the higher temperature the TL peak, which is not completely record-able.

The behavior of the peak height (I_m), which is the most common measure of the experimental TL data, is found to be superlinear. This new result in the OTOR model could have serious implications for dosimetric applications, because it violates the equivalency between peak height and peak integral in TL applications. This superlinear behavior is also due to the violation of QE assumptions and the distortion of the shape of the TL peak.

The lifetime of electrons in traps within the OTOR model depends strongly on the trap filling ratio n_0/N . In the low dose region and during irradiation with low dose rates, the effective lifetime can increase dramatically, due to retrapping events dominating over recombination processes.

One of the main assumptions of the phenomenological OTOR model is that electron and hole traps are not created by irradiation, but rather preexist in the material. These empty traps and centers are filled during irradiation. In future work we intend to examine this assumption, and study the behavior of a material at very low dose rates and doses, when the “electron–hole pairs” are created by the irradiation process itself.

Declaration of competing interest

The authors declare that they have no known competing financial interests or personal relationships that could have appeared to influence the work reported in this paper.

Data availability

Data will be made available on request.

References

- Chen, R., 1969. On the calculation of activation energies and frequency factors from glow curves. *J. Appl. Phys.* 40, 570–585.
- Chen, R., Huntley, D.J., Berger, G.W., 1983. Analysis of thermoluminescence data dominated by second-order kinetics. *Phys. Stat. Sol. (A)* 79, 251–261.
- Chen, R., Pagonis, V., 2011. *Thermally and Optically Stimulated Luminescence: A Simulation Approach*. John Wiley & Sons, Chichester.
- Chen, R., Pagonis, V., 2013. On the quasi-equilibrium assumptions in the theory of thermoluminescence (TL). *J. Lumin.* 143, 734–740.
- Chen, R., Pagonis, V., Lawless, J.L., 2010. Nonlinear dose dependence of TL and LM-OSL within the one trap–one center model. *Radiat. Meas.* 45, 277–280.
- Furetta, C., Kitis, G., 2004. Review models in thermoluminescence. *J. Matter. Sci.* 39, 2277–2294.
- Garlick, G.F.J., Gibson, A.F., 1948. The electron trap mechanism of luminescence in sulfide and silicate phosphors. *Proc. Phys. Soc. Lond.* 60, 574–590.
- Kitis, G., 2020. Theory and practice of the methods used to evaluate the physical parameters of electron trapping levels. In: Dhoble, S.J., Chopra, V., Nayar, V., Kitis, G., Poelman, D., Swart, H.C. (Eds.), *Radiation Dosimetry Phosphors*. Elsevier WP, pp. 129–156.
- Kitis, G., Chen, R., Pagonis, V., 2008. Thermoluminescence glow-peak shape methods based on mixed order kinetics. *Phys. Stat. Sol. (A)* 205 (5), 1181–1189. <http://dx.doi.org/10.1002/pssa.200723470>.
- Kitis, G., Pagonis, V., 2007. Peak shape methods for general order thermoluminescence glow-peaks: A reappraisal. *Nucl. Instr. Meth. Phys. Res. B* 262, 313–322.
- Kitis, G., Pagonis, V., 2017. New expressions for half life, peak maximum temperature, activation energy and kinetic order of a thermoluminescence glow peak based on the Lambert W function. *Radiat. Meas* 97, 28–34.
- Kitis, G., Vlachos, N.D., 2013. General semi-analytical expressions for TL, OSL and other luminescence stimulation modes derived from OTOR model using the Lambert W - Function. *Radiat. Meas* 482, 47–54.
- Lovedy Singh, L., Gartia, R.K., 2013. Theoretical derivation of a simplified form of the OTOR/GOT differential equation. *Radiat. Meas.* 59, 160–164.
- May, C.E., Partridge, J.A., 1964. TL kinetics of alpha irradiated alkali halides. *J. Chem. Phys.* 40, 1401–1409.
- Randall, J.T., Wilkins, M.H.F., 1945a. Phosphorescence and electron traps I. The study of trap distributions. *Proc. R. Soc. London* 184, 366–389.
- Randall, J.T., Wilkins, M.H.F., 1945b. Phosphorescence and electron traps II. The interpretation of long-period phosphorescence. *Proc. R. Soc. London* 184, 390–407.
- Sadek, A.M., Eissa, H.M., Basha, A.M., Kitis, G., 2014. Resolving the limitation of peak fitting and peak shape methods in determinations of the activation energy of thermoluminescence glow peaks. *J. Lumin.* 146, 418–423.
- Sadek, A.M., Kitis, G., 2017. A critical look at the kinetic parameter values used in simulating the thermoluminescence glow-curve. *J. Lumin.* 183, 533–541.